

# Cryo-FIB-lift-out: practically impossible to practical reality

CHRISTOPHER DAVID PARMENTER\*  & ZUBAIR AHMED NIZAMUDEEN\*, †

\*Nottingham Nanoscale and Microscale Research Centre, University of Nottingham, Nottingham, UK

†Division of Cancer and Stem Cells, Nottingham Biodiscovery Institute, The University of Nottingham, Nottingham, UK

**Key words.** Beam-sensitive, biological sample preparation, cryo-FIB, Lift-Out, soft-matter.

## Summary

In this paper, we explore the development of the Cryo-Lift-Out (cryo-LO) technique as preparation tool for cryogenic transmission electron microscopy (cryo-TEM). What started in early work defying what was considered ‘practically impossible’ has developed into state-of-the-art practical reality. This paper presents the key hardware, basic principles and key considerations for the practical usage of cryogenic Lift-Out for those new to the field. Detailed protocols and in-depth description of considerations and points for further development are presented. The authors have attempted to formalise everything known about the technique gathered together from their expertise gained in the development of this approach.

## Introduction

A long-standing dream of electron microscopists is observing the functionality of macromolecular complexes within a living cell. High-end transmission electron microscopes (TEM) are suitable to distinguish macromolecular complexes, but TEM relies on advanced sample preparation strategies. Ultramicrotomy has traditionally been the preferred method of choice for thin section preparation; however, it suffers recognised artefacts arising from compression, cutting and thickness variations (Dubochet *et al.*, 2007; Han *et al.*, 2008). Cells must be frozen to a vitreous state and kept frozen, resulting in very fragile sample material.

The first paper to show that the use of a Focused Ion Beam (FIB) does not cause devitrification of ice dates back to 2006 (Marko *et al.*, 2006). A number of cryo-FIB-based approaches have been developed since, using different strategies to produce thin sections, called lamella, from hydrated, frozen samples (Marko *et al.*, 2006; Hayles *et al.*, 2010; Rigort *et al.*, 2010; Parmenter *et al.*, 2016). With the realisation that the FIB-Scanning Electron Microscope (FIB-SEM) presents realistic

alternatives for TEM preparation, there has been a shift in thinking that it is perhaps the only technique currently available for producing samples from cells and tissue in a minimally altered state (Edwards *et al.*, 2009; Rigort & Plitzko, 2015).

One traditional FIB-SEM approach is the preparation and separation of a lamella from a region of interest in a bulk sample (site-specific preparation) followed by its transfer to a TEM. This approach known as ‘Lift-Out’ has been applied in the fields of semiconductors (Krueger, 1999) and materials science (Giannuzzi *et al.*, 1998; Sivel *et al.*, 2004; Li *et al.*, 2006). The regular (i.e. room temperature) application of this technique requires not only a FIB-SEM but also a micromanipulator for removal of the lamella, either operated *in situ* in the vacuum of the FIB or *ex situ* as a standalone instrument (Giannuzzi *et al.*, 2015). The lamella is sometimes known as a foil or membrane. Once suitably thin, the lamella is mounted on a specialised support grid and can be transferred to the TEM for further imaging and analysis (Fig. 1).

Performing the Lift-Out procedure under cryogenic conditions adds significant complications. The sample must be maintained at cryogenic temperatures and the micromanipulator should also be cooled to a similar temperature to avoid sample damage or alteration. These two factors, coupled with the fact that the sample should be maintained free from environmental moisture, mean that any use of the manipulator must be done inside the FIB-SEM, making *in situ* extraction the only option. These challenges increase the difficulty to the point where it was considered impossible or unfeasible for practical application. As a result, alternative approaches were prioritised including the ‘on-grid’ thinning technique (Rigort *et al.*, 2010; Rigort *et al.*, 2012) and cryothinning of high-pressure frozen samples (Marko *et al.*, 2007; Hayles *et al.*, 2010; Hsieh *et al.*, 2014). The state-of-the-art for such approaches are reviewed here (De Winter *et al.*, 2020; Kuba *et al.*, 2020).

Early published work delivered cryogenic-Lift-Out (cryo-LO) on a lamella mounted to a copper support post using platinum deposition (Rubino *et al.*, 2012) or water from the Selective Carbon Mill GIS (Gas Injection System) (Parmenter *et al.*, 2014), through a combination of hardware modifications

Correspondence to: Christopher Parmenter, Senior Research Officer in Cryogenic Electron Microscopy, Nottingham Nanoscale and Microscale Research Centre, University Park Campus, Nottingham, UK. Tel: 0115 84 68943; e-mail: christopher.parmenter@nottingham.ac.uk

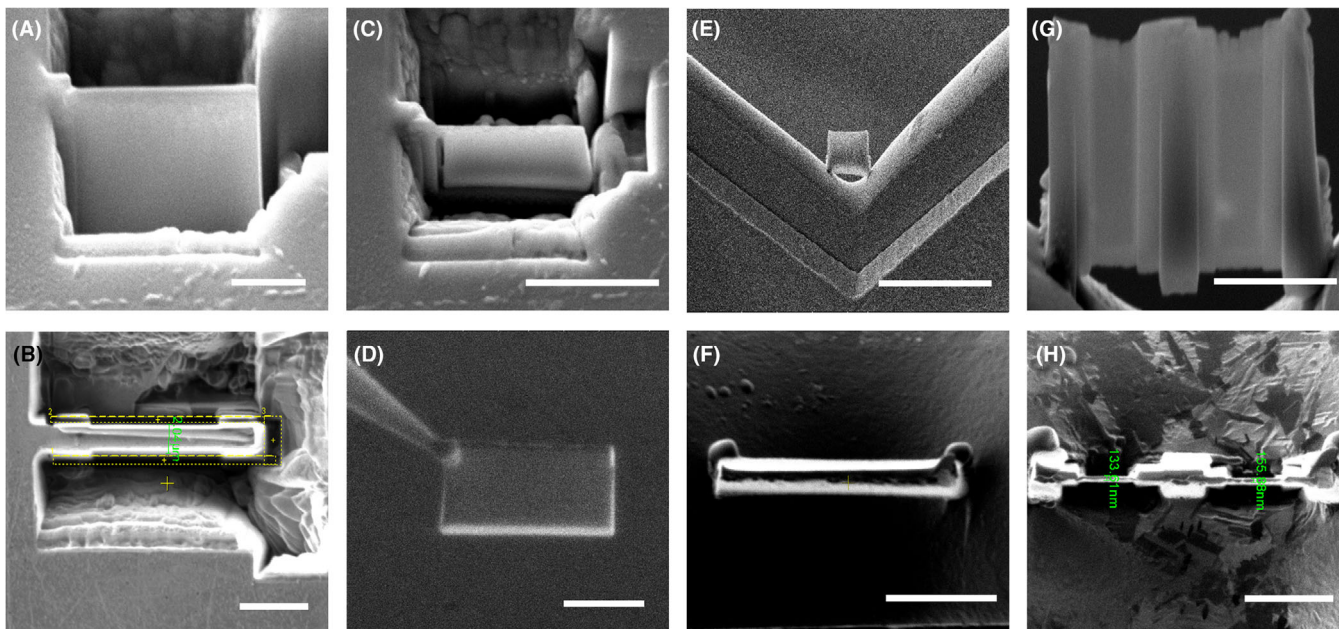


**Fig. 1.** A lamella (also known as a foil or membrane) prepared for Lift-Out. Top row SEM view, bottom FIB view. (A), (B) Thinning of the lamella. (C) The FIB ‘undercut’ is made prior to attaching the micromanipulator needle to the lamella (not shown). (D) The lamella is transferred to the support grid by the micromanipulator. (E), (F) The lamella is mounted on the support grid in the so-called V-post by depositing a platinum precursor gas with the FIB. (G), (H) The sample is thinned to electron transparency prior to TEM. Scale bars (A), (B), (D), (F), (G) 5  $\mu\text{m}$ . (C) 10  $\mu\text{m}$ . (E) 30  $\mu\text{m}$ . (H) 3  $\mu\text{m}$ .

and the development of handling protocols. Successful transfer and imaging in a cryo-TEM was viewed as a significant achievement and that cryo-LO had become a potential option. Since that work, the technique has been demonstrated to work for different samples including spores, hydrogels, yeast and tissue (Rubino *et al.*, 2012; Parmenter *et al.*, 2014; Mahamid *et al.*, 2015; Schaffer *et al.*, 2019). The cryo-LO approach can of course be applied to any sample in the FIB-SEM, subject to the cooled stage and manipulator being present and this has been evidenced in the case of hard–soft interfaces such as battery materials (Zachman *et al.*, 2016).

What follows is a detailed look at the hardware, considerations and protocols that must be employed for this approach to be successfully undertaken.

## Methods and materials

### Sample

Most experimental details reported in this paper and the application of the procedure are mainly using a ‘test sample’ of baker’s yeast (*Saccharomyces cerevisiae*), a readily available, simple to prepare, well studied organism.

### Sample preparation

Samples for cryo-FIB may be prepared in a range of ways depending on water content and size. Preparation methods

include high-pressure freezing (HPF) (Moor, 1987), ethane plunging (Tivol *et al.*, 2008), metal mirror (MM) (Livesey *et al.*, 1991) and nitrogen slush (LN<sub>2</sub> slush) (Umrath, 1974). Of key importance is the preservation of the native state of the sample at macromolecular level. Thus, a glassy or vitreous freezing is preferred (Dubochet, 2007) in avoidance of ice crystal formation.

Nitrogen slush freezing has a lower freezing rate but has been generally accepted for cryo-SEM. Ice crystals and damage caused by ice crystals are of little concern when imaging fracture surfaces with SEM resolutions. Where the ultimate destination is the TEM, however, the formation of ice crystals should be avoided wherever possible as it can be assumed that these will damage structures within the sample (ultrastructural damage) and their presence will obscure or deform features of interest. For a more thorough exploration of this topic, see Hayles & de Winter (2020).

Plunge freezing of samples with low water content into nitrogen slush will suffice to bring the sample into a vitreous status. Slower cooling in the cryochamber is an option if samples (bitumen) suffer thermal shock in liquid nitrogen or in the case of polymeric, where water content could be zero and ice crystal formation is of little concern. In this work, hydrogels and yeast (*S. cerevisiae*) samples were frozen by metal mirror freezing to a vitreous state, thus preserving ultrastructure (Livesey *et al.*, 1991; Reipert *et al.*, 2003).

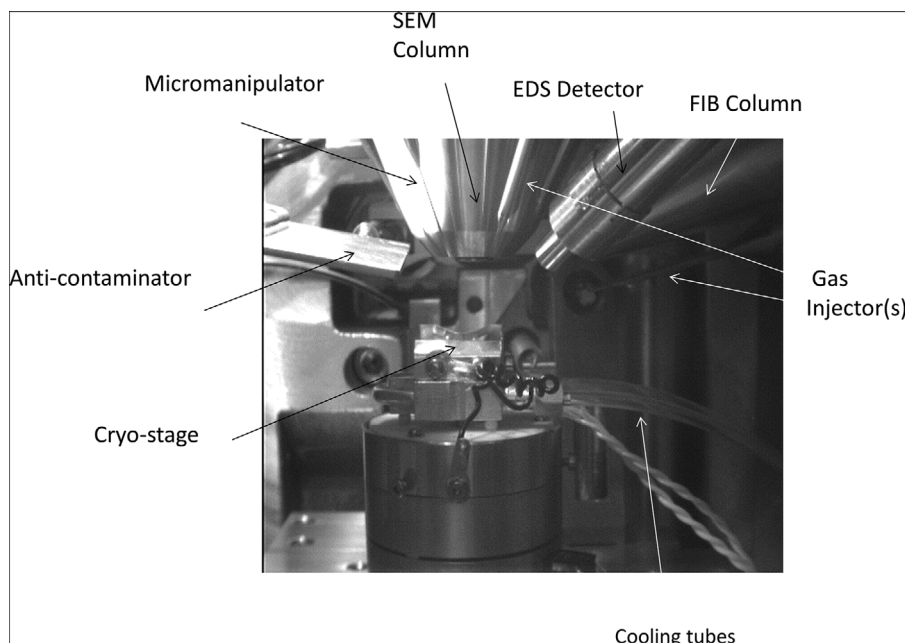


Fig. 2. A view inside the microscope chamber reveals the main required components of a FIB-SEM for cryo-LO, including the cryostage, the micromanipulator and the gas deposition system (GIS) injectors.

### Instrumentation

The exact instrumentation used for cryo-LO hardware will differ based on the combination of microscope manufacturers, stages and micromanipulators from lab to lab, but the systems broadly consist of the following:

- FIB-SEM capable of imaging (SEM) and milling (FIB)
- Cryogenic stage capable of maintaining the sample at cryogenic temperatures (ideally below  $-150^{\circ}\text{C}$ )
- Cooled micromanipulator (this will be a modification from the typical room temperature version, supplied by vendor but should be as cold as the sample).
- Gas Injection System (GIS) for the attachment of the lamella to the manipulator and to the support grid. The most used systems for cryo-FIB is a platinum precursor gas (Pt GIS) or water [Selective Carbon Mill (SCM GIS)]. The SCM GIS is referred to as water GIS.
- A sample holder (sledge/shuttle) which needs to be capable of supporting the sample and Lift-Out grid. This could be custom made or a supplied commercial holder.

The FIB-SEM used in this paper is a Quanta 200 3D FIB-SEM (FEI/ThermoFisher, Hillsboro, OR, USA) operated at an accelerating voltage of 5–15 keV (electron beam) and 30 kV (ion beam). The samples were maintained at cryogenic temperatures of  $-170^{\circ}\text{C}$  using a Quorum 3010 Cryostage (Quorum Technologies, Loughton, UK) with the anti-contaminator run at  $-194^{\circ}\text{C}$  which supplied cooling to a cryomicromanipula-

tor (Omniprobe100, Oxford Instruments, High Wycombe, UK) (Fig. 2).

Cryo-TEM was performed using a JEOL 2100+ equipped with Gatan 626 cryoholder. Bright-field TEM Images were collected using a Gatan US1000XP CCD camera and STEM images were collected using JEOL bright-field and dark-field STEM detectors.

### Outline of procedure

A yeast sample is frozen by metal mirror freezing to provide a flat, vitreous frozen sample, ideal for cryo-LO. The sample is secured onto a cryosledge and transferred to the cryopreparation chamber where the sample is sputter coated with a few nano meters of platinum to make it more electrically conductive. The coated sample is transferred to the cryostage (in the main SEM chamber) at  $-170^{\circ}\text{C}$ . Once a suitable site is identified, the Pt GIS is used to deposit approximately a  $2\ \mu\text{m}$  thick layer (Hayles *et al.*, 2007). Pt deposition is crucial to prevent FIB exposure of the area of interest and to reduce curtaining artefacts on the FIB-milled face of the material.

The lamella is oriented perpendicular to the sample surface, which requires the sample to be tilted  $52^{\circ}$  towards the FIB. Trenches are initially milled at a current of 1–3 nA, followed by a further thinning step with a current of 0.5 nA, yielding a lamella suitable for extraction. The lamella is undercut after tilting the stage back to  $0^{\circ}$ . Both the cooled micromanipulator probe and the water GIS are inserted. The cooled micromanipulator probe is positioned such to make contact with the

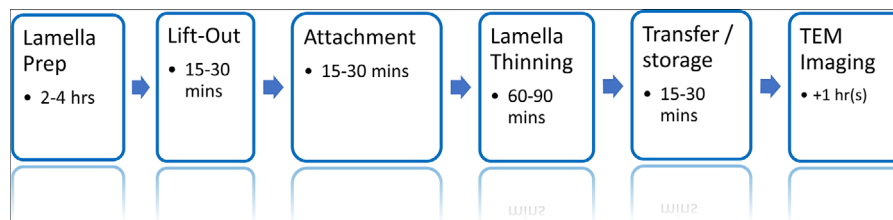


Fig. 3. Overview of the steps and approximate time required to produce, extract, attach, thin and transfer to the cryo-TEM.

lamella. The water GIS nozzle is opened for approximately 10 seconds until a layer of ice is observed between the lamella and the micromanipulator. Once the two surfaces are joined, the final link between the lamella and the bulk is cut with the FIB. The lamella is carefully lifted away from the bulk and transferred to a cooled support grid. The lamella is secured against the cooled support grid by again using water deposition. The lamella can be thinned at lower currents with care being taken that the cryocondensed gas (water or Pt) is not milled excessively at the point(s) of joining. Care should be taken to preserve the Pt protection layer at the top of the lamella (previously deposited before milling began). If this layer is damaged, uneven milling will result in substantial ‘curtaining’ in the finished lamella. Once the lamella has been extracted, attached to the support grid and thinned, the lamella is ready for transfer to a precooled cryo-TEM holder. Transfer to a storage facility is also an option, but poses the risk for the lamella to collect contamination from liquid nitrogen-born ice balls (Hayles *et al.*, 2020).

The entire procedure can be summarised in a schematic of the major steps and approximate times for each step required. The overview and schematic (Fig. 3) downplay the complexity of the technique. The remainder of this paper attempts to convey the protocols, details and issues to consider when trying to perform the ‘practically impossible’.

### The cryo-FIB-SEM procedure in full

#### Preparing yeast

A yeast sample is reactivated for 20 min in tap water to make a thin paste. Approximately 10  $\mu\text{L}$  of the paste is placed into a metal ring stuck to a double-sided copper tape on a metal mirror freezing sponge. The yeast is frozen using a metal mirror freezer (Leica MM80, Leica Microsystems, Vienna, Austria) by a rapid plunge onto a liquid nitrogen cooled metal block.

#### Transfer to the microscope chamber

The sample is moved to the slushing pot of the QT3010 system and mounted onto a specific purpose-built sledge suitable for cryo-LO. The mounting of small samples onto a sledge is done manually with tweezers underneath liquid nitrogen, which requires some practicing prior to the first experiment. Once

mounted, the cryotransfer-shuttle transfers the sample under vacuum conditions to the preparation chamber. The stage in the preparation chamber is held at  $-170^\circ\text{C}$  to ensure that vitreous ice is preserved. Once in the preparation chamber, samples must then be sputter coated with platinum, to make the sample conductive for SEM imaging. Standard conditions used are a current of 10 mA for 60 s in an argon environment at  $\sim 1 \times 10^{-2}$  mbar pressure, by bleeding in argon controlled by the Quorum software. Following successful sputtering, the sample is transferred into the main sample chamber and docked into the cryostage, which is at the same temperature as the prep chamber ( $-170^\circ\text{C}$ ). Details of the transfer and sputter coating will vary between systems. For example, Leica has an off column cryoprep chamber and ThermoFisher has an in-chamber sputter coater.

#### Temperature conditions

With the cryostage set to  $-170^\circ\text{C}$ , the anti-contaminator is typically set to  $-194^\circ\text{C}$ . It must be noticed that the temperature at the sample surface or the anti-contaminator can be higher than measured by the sensor. Two pieces of metal held together tightly by screws can still lose  $5\text{--}10^\circ\text{C}$ . Therefore, it is advised to calibrate your instrumentation, as a systematic temperature difference can be present, depending on the location of the sensor and the complexity of the construction. To avoid devitrification, some systems are advised to be operated at much lower temperatures ( $-194^\circ\text{C}$ ). Ultimately the sample must remain below  $-138^\circ\text{C}$  and the anti-contaminator is kept  $20\text{--}30^\circ\text{C}$  lower. A much colder anti-contaminator will lower the partial water vapour pressure in the microscope chamber which increases the sublimation rate of the sample (Hayles *et al.*, 2020). This is in particular potentially risky for a 100 nm thin lamella that remains in the chamber for many hours. With the sample safely in place, the next step is Pt deposition.

#### Pt deposition

The stage is lowered 0.5–3.5 mm (depends on the microscope being used) below the standard FIB-SEM working distance (‘eucentric height’) and the Pt GIS is inserted, when the area of interest is located. The Pt GIS contains a standard precursor gas and is available on many FIB systems, either as a

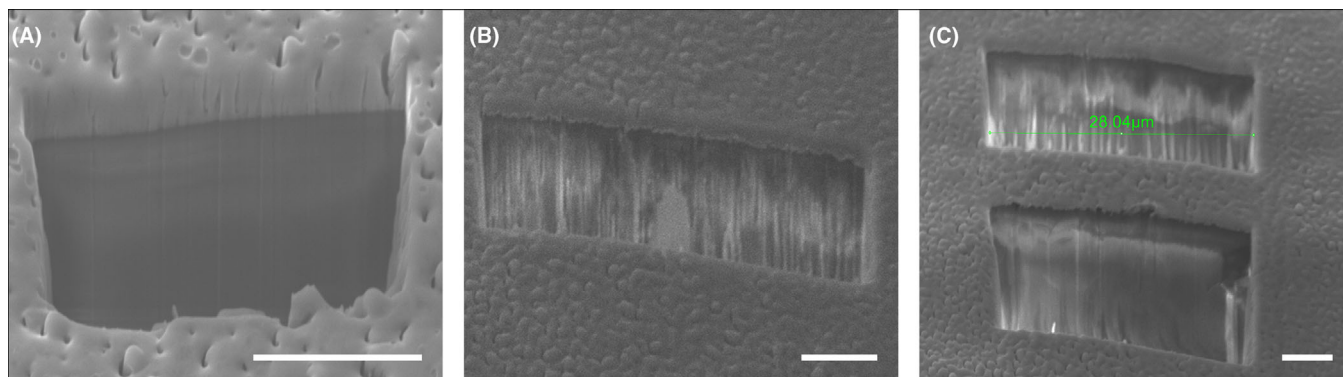


**Fig. 4.** (A), (B) SEM images showing the platinum layer and the sample below. (C) SEM image following the second cut leaving the beginning of a lamella. Scale bars (A) 10  $\mu\text{m}$ , (B), (C) 5  $\mu\text{m}$ .

standalone crucible or as part of a multi-crucible system. The Pt GIS should be set to a deposition temperature of 27°C and warmed in advance, as outlined by Hayles *et al.* (2007). Opening the nozzle and allowing approximately 10–15 seconds of gas flow should be enough to deposit a layer of approximately 2  $\mu\text{m}$  thick Pt organometallic over the sample. The duration of deposition and positioning distance of the GIS is specific to each FIB-SEM and so some testing on a dummy sample is required, prior to the first real experiment. Once the GIS valve is closed, the GIS is withdrawn, and the sample returns to the original working height.

The platinum deposition layer must be exposed to the FIB beam. Typically, an exposure from a beam of 1 nA for 20–30 s is enough to make the contrast change from dark to light, resulting in a smooth looking surface. This signifies that the first cut can be made. A test cut is advised as to check whether the deposition worked according to plan as outcomes may differ depending on the sample material. Suggested milling currents are 1–3 nA, 5 nA for larger volumes on soft materials, depending on damage limits and volume of materials to be removed.

Following a successful first cut, a cross-section of the sample should now be visible in the SEM image window. A clearly visible layer of platinum deposition (1–3  $\mu\text{m}$ ) should be visible, as shown in Figure 4.

#### *Preparing a lamella*

The test cut is expanded using currents of 1–3 nA. Subsequent lower currents 0.5–0.3 nA serve to polish the face of the cross-section. The second large cut is positioned behind the initial one and generally larger in the direction away from the lamella. An increased length of the trench is advantageous when the sample is tilted back to 0° and the undercut is milled. As a ballpark figure, we cut back approximately twice the desired height (depth in  $z$ ) of the lamella. Once the two cuts are complete, a lamella of unmodified material remains, which should be approximately 3–5  $\mu\text{m}$  in thickness (Fig. 4C). The thickness can be reduced prior to Lift-Out; however, the ar-

range of the cooled micromanipulator and GIS injectors must be considered when milling the lamella.

#### *Lamella extraction methods*

Recently, several solutions have been proposed for effective extraction of a lamella under cryoconditions including those with prototype hardware developed with manufacturers (Rubino *et al.*, 2012; Parmenter *et al.*, 2014; Mahamid *et al.*, 2015). Two options are discussed below, which represent commercially available solutions from Oxford Instruments and Kleindiek (Kleindiek Nanotechnik, Reutlingen, Germany). One involves the Omniprobe micromanipulator, a sharp, cold needle. The other involves a cold, Kleindiek micromanipulator gripper.

The micromanipulator temperatures should ideally be at the same temperature as the sample, but at least  $-138^\circ\text{C}$ , the devitrification temperature of vitreous ice. Current commercially available systems are reported to operate around  $-160$  to  $-165^\circ\text{C}$  and this cooling is typically delivered from the anticontaminator via a metal braid.

The two methods also serve as an overview of the procedures required to perform cryo-LO for those wishing to attempt their own cryo-LO. There will be differences between these details and those required for installations on other systems; however they should be broadly applicable.

#### *Cryo-LO with an Omniprobe*

*Attaching the needle.* The micromanipulator of the microscope is a key component to enable Lift-Out of the lamella from the bulk sample. The Omniprobe cryo-micromanipulator (Omniprobe) is a retrofitted Omniprobe 100.7 and is the commercially available version of the prototype developed for the initial work published in 2014 (Parmenter *et al.*, 2014) and 2016 (Parmenter *et al.*, 2016). Attachment of the micromanipulator to the lamella is performed by the application of a gas phase substance (typically water or a complex containing

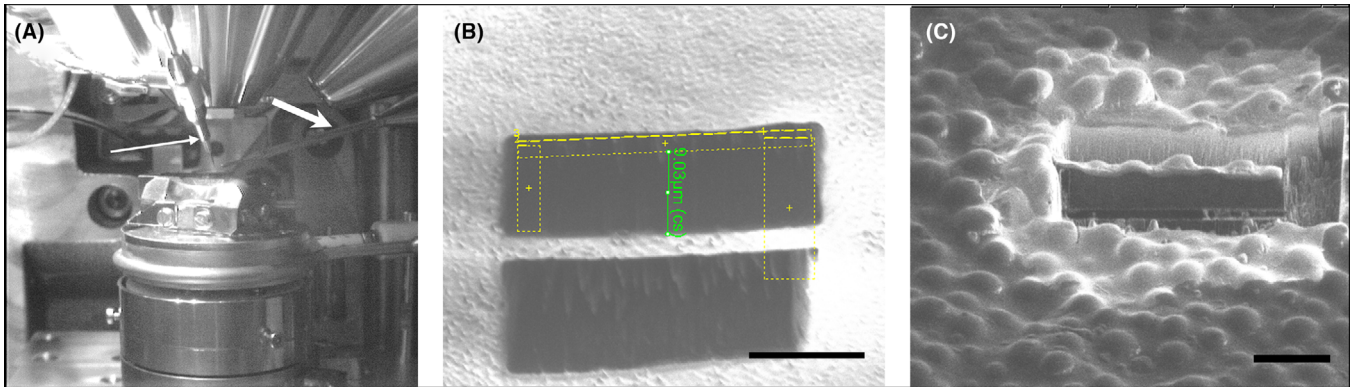


**Fig. 5.** (A) The stage position during the final preparations for the Lift-Out. The thick white arrow indicates the water GIS and the thin white arrow indicates the cryo-Omniprobe. (B) The milling of a J-cut (undercut) shown from ion beam view (milled in parallel). (C) A lamella resulting from the J-cut and ready for extraction. Scale bars 10  $\mu\text{m}$ .

platinum), which attaches (cryo-condenses) to both the lamella and manipulator. The GIS crucible must be heated in advance of deposition and heated to the correct temperature for cryo-usage (27°C for Pt and 28°C for water).

Once the basic lamella has been milled, the sample is tilted to an angle of 0° to perform a series of undercut and side-cuts (so-called J-cut) in order to free it from the bulk material (Fig. 5). The exact dimensions of the under and side-cuts are suggested to be at least 1  $\mu\text{m}$  wide to avoid reattaching the lamella to the bulk when attaching the manipulator. This reattachment can arise from redeposited material when milling these cuts or due to cryo-condensation of water or platinum while attempting to attach the manipulator to the lamella.

The side on which the manipulator approaches is cut wider (2–4  $\mu\text{m}$ ) compared with the non-manipulator side. The wider cut prevents reattachment from cryo-condensing excess deposition gas while attaching the micromanipulator to the lamella. If the GIS is on the opposing side to the manipulator, this larger cut may be less crucial; however, some experimentation is suggested to ensure smooth attachment and release of the lamella. The side of the lamella still attached to the bulk sample should be cut until just below the top of the lamella, but leaving a small volume still attached to the bulk sample (Fig. 5B).

**Extraction.** Following preparation for extraction, the stage (at 0° tilt) is dropped by a few millimetres and both the manipulator and GIS are inserted, ensuring that the GIS crucible is set to the correct temperature. It is possible to understand the 3D position and orientation of the stage (sample), the GIS and manipulator by utilising the different SEM and FIB low current imaging facilities. Details of micromanipulator navigation vary per system and per installation. In principle, the micromanipulator is gently pushed against the lamella (Figs. 6B,C). At the point where the micromanipulator touches the lamella, on the side or top there may be a change of contrast

due to a change in conductivity as the sample is grounded through the manipulator. The contrast change serves as additional reassurance that there is contact. The GIS is now activated for approximately 10 s to deposit the chosen gas, thereby attaching the lamella to manipulator (Fig. 6D). The exact timing may vary per instrument and requires some testing prior to working with the actual sample of interest. Once the lamella is attached, it may be necessary to remill the under and side cuts if deposited gas has filled the cuts significantly. The final cut of the lamella should be the last remaining connection between the lamella and bulk (Fig. 6E), which was previously left intentionally unmilled. Cutting the lamella free should be done swiftly (300–500 pA), as any manipulator or stage movement could lead to loss of the lamella. It may be possible to see the lamella detach from the bulk during the final cut and this may be accompanied by a change in contrast as before. Once the lamella is detached, return to a low current ion beam current (30–50 pA) and make a small, slow movement of the lamella in the  $x$ -axis to see if the lamella separates from the bulk. If a successful separation is confirmed, the stage is moved away (down) from the micromanipulator. This should reveal the lamella on the tip now free of the bulk (Fig. 6F). At this point some users may desire to add additional attachment gas for reassurance.

**A note on the GIS and manipulator arrangement.** Seemingly trivial, the arrangement of the GIS and the micromanipulator is actually very important. If the GIS delivering the attachment gas is on the opposite side of the cooled probe (Fig. 7A) then the micromanipulator should be attached to the top of the lamella to be extracted (Figs. 8A,B). This will allow gas to condense around the tip and lamella. However, if the GIS containing the gas is in a similar oriented port (same side) to the micromanipulator (Fig. 7B), it is likely that the gas cannot condense between the surfaces, meaning that attachment will be very difficult. In this case the micromanipulator should be positioned to the side of the lamella so that the gas can

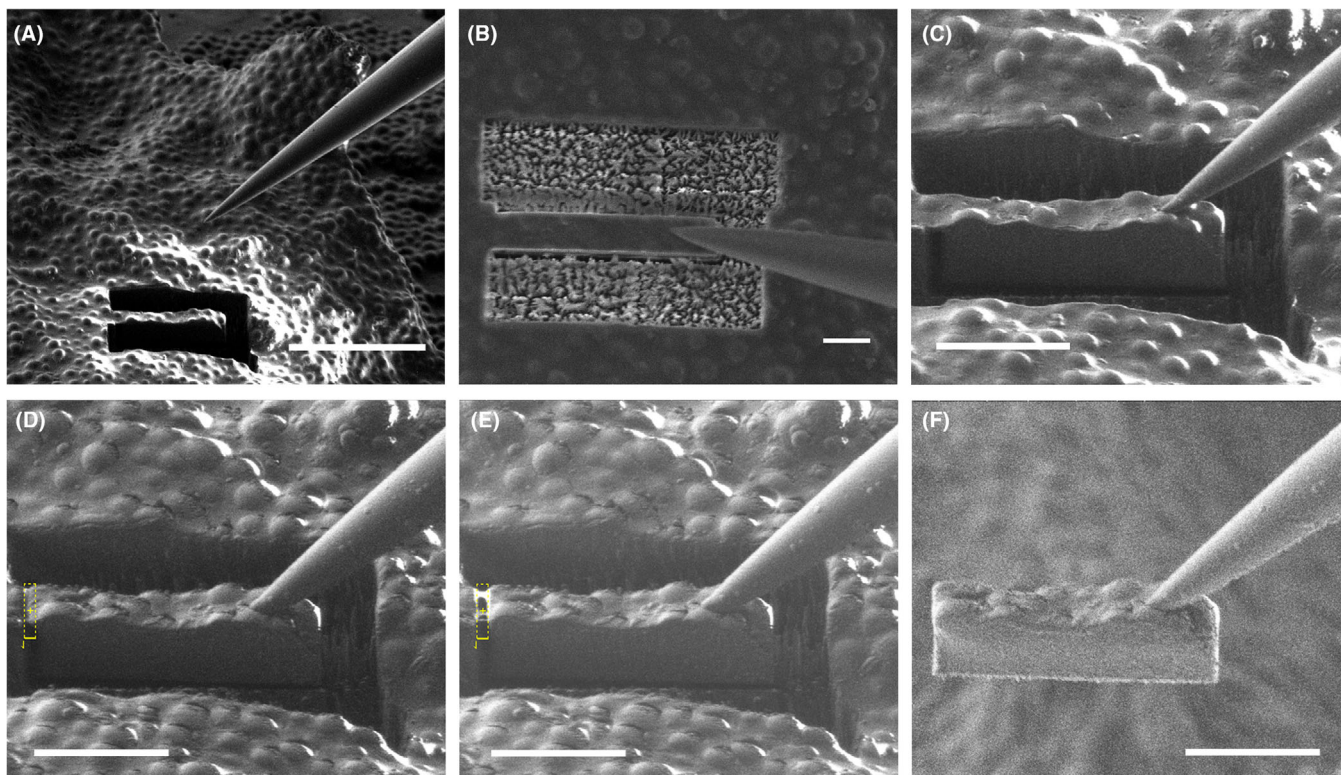


**Fig. 6.** A complete overview of the Lift-Out procedure. (A) The approach of the micromanipulator using the FIB window. (B) The positioning of the micromanipulator is monitored top down by the SEM. (C) Making contact with the lamella. (D) Deposition from the water GIS to attach the micromanipulator to the lamella. (E) Milling away the last remaining connection between the bulk sample and the lamella. (F) The lamella secured to the tip of the Omniprobe, free from the bulk.

condense between the top of the micromanipulator and the side of the lamella (Fig. 8C). The destination of the lamella, whether the lamella is to be attached to the right or left of a post is also a consideration when deciding how to attach the micromanipulator.

*Lamella deposition to LO-grid.* The micromanipulator is withdrawn, along with the GIS. The stage is moved to the position of a dedicated TEM Lift-Out grid (LO-grid), sometimes called 'half-grid' or 'C-mount'. A LO-grid is half a ring (outer diameter 3 mm) with several posts in the middle. Some designs

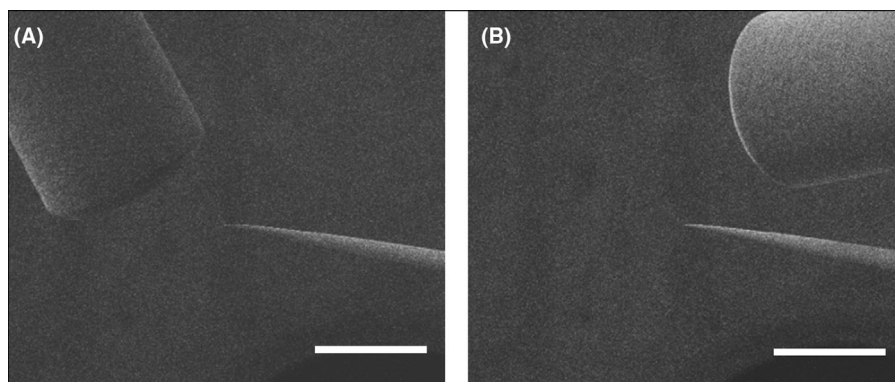


**Fig. 7.** The relation of the micromanipulator to the (A) water GIS and (B) Pt GIS. The positions relate to a FEI Quanta 3D chamber; however, the concept of same side/opposite should be generally valid. Understanding the relationship of these objects and their relation to the lamella and the LO-support grid is critical to secure attachments at extraction and mounting. Scale bars 500  $\mu\text{m}$ .

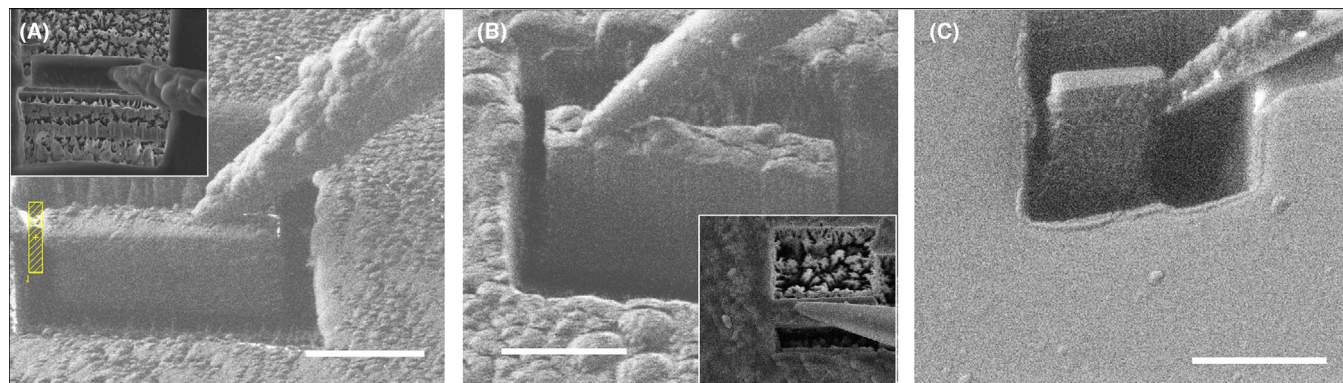


**Fig. 8.** The lamella is attached to the Omniprobe by the water GIS. (A) on the right side and (B) on the left side. The insets in (A) and (B) show the SEM view of the same lamella. (C) The Omniprobe is positioned to the right of the lamella. Note the larger gap on the right of the lamella required to accommodate the manipulator. Scale bars 10  $\mu\text{m}$ .

contain V-shaped posts as well as pillars. The lamellae are usually mounted on top of the posts or to the side of the post. Most LO-grids are made from copper but are available from other materials as well (nickel, molybdenum, gold, stainless steel, titanium, aluminium).

At this point, it may be necessary to move the sample stage to a point where the sample sledge can be unloaded and replaced with a preloaded LO-grid. Alternatively, the sample and LO-grid can be incorporated into a single sledge. The latter allows more straightforward usage and reduces two steps in the procedure. In either case, move both the stage to the LO-grid position in preparation for attachment of the lamella to the LO-grid and detachment of the lamella from the micromanipulator. Ensure the stage is below eucentric height and insert the GIS and the micromanipulator. Carefully raise the stage height and use low-current SEM and FIB imaging to bring the lamella alongside the selected post of the LO-grid. Making contact between the lamella and the LO-grid must be done gently. Once in contact at the appropriate height along the post, GIS deposition (water or Pt) attaches the lamella and LO-grid together (deposition time approximately 10 s). The final step is cutting the micromanipulator free from the lamella with a medium current (300–1000 pA) Figure 9 demonstrates the steps of approaching the LO-grid (Fig. 9A) for both side-of-post (Figs. 9B, C) and V-shaped post examples (Figs. 9D–F).

#### *Lamella extraction using Kleindiek gripper*

**Picking up the lamella.** An alternative approach to the use of a cooled micromanipulator is a cooled gripper (Schaffer *et al.*, 2019), which is a modification to the standard room temperature Kleindiek gripper (Kleindiek Nanotechnik). The approach has been demonstrated on a  $45^\circ$  pretilted holder that holds the sample and the LO-grid, but at different angles. For lamella extraction, the stage tilt is therefore significantly different to that described for the Omniprobe approach; however the stage tilt to  $7^\circ$  results in the sample to be milled being perpendic-

ular to the ion beam, ( $45^\circ + 7^\circ = 52^\circ$ ) as is normal for FIB milling. Lamella preparation proceeds in a similar way and following undercutting, the gripper is inserted, opened and centred over the prepared lamella. The gripper is then lowered in the  $z$ -axis guided by live electron beam imaging. Once successfully gripped, the final milling is done to free the lamella from the bulk sample using the ion beam. Lift-Out is performed by moving the gripper along the  $z$ -axis.

**Lamella deposition.** After the Lift-Out, the stage is lowered to ensure it does not pose a risk to the gripper, before rotation of the stage to the 'lamella insertion' position. The stage is moved to a premilled 'pocket' on the LO-grid, and the lamella is brought close to the slot. To release the lamella, the gripper is opened, such that the lamella remains attached to one of the gripper's 'fingers' (i.e. prongs) by passive adhesion and electrostatic forces. The lamella is carefully lowered completely into the slot. To fully detach the lamella from the gripper, a slight movement of the stage is required before the micromanipulator is retracted. To secure the lamella, organometallic platinum is deposited using the GIS.

#### *Lamella thinning*

Once the lamella is attached to the LO-grid, the excess deposited ice/organometallic platinum which encases the lamella needs to be removed (Figs. 10A–D). The FIB mills away the excess material and continues thinning the lamella to electron transparency (200–300 nm). Milling currents starting at 500 pA and finishing at 50–30 pA provide careful removal of excess materials in a reasonable time frame. Care should be taken to avoid any cryo-condensed materials that attach the lamella to the LO-grid post or the entire lamella could be lost (Fig. 10C). The use of over and under tilting ( $\pm 2^\circ$  or more) ensures parallel surfaces on either side of the lamella. As has been described at length, the entire Lift-Out procedure is complex. It can be summarised in the following workflow

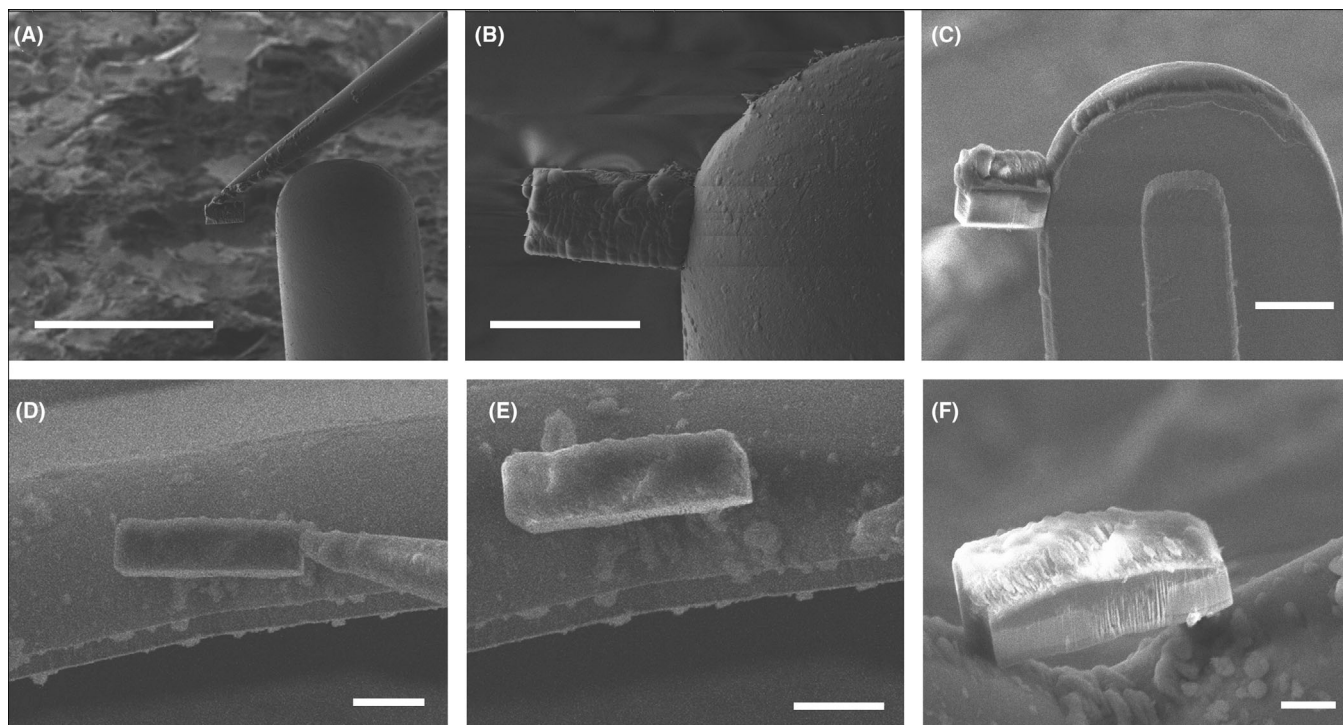


**Fig. 9.** Different options to mount a lamella to the LO-grid. (A) The approach of the micromanipulator towards the LO-grid. (B) The lamella is attached to the side of the LO-grid post by water deposition (FIB image). (C) Same as (B) but imaged by the SEM. (D) A lamella being mounted in the V-shaped post. (E) The lamella is attached to the LO-grid and the micromanipulator is released. (F) Same as (E) but imaged by the SEM. Scale bars (A) 100  $\mu\text{m}$ , (B), (C) 20  $\mu\text{m}$ , (D), (E) 10  $\mu\text{m}$ , (F) 5  $\mu\text{m}$ .

diagram (for an Omniprobe-based procedure) (Fig. 11) which has been colour coded for easier understanding.

#### Transfer to the TEM

The shuttle/sledge carrying the LO-grid is moved into the prep chamber (if available) via the transfer rod, where platinum sputter coating may be applied optionally to increase the conductivity of the lamella. The sample is then moved under vacuum into transfer chamber (which is common to all transfer rods). This protects the shuttle from moisture during its movement from the airlock of the prep-chamber into a liquid nitrogen filled sample prep unit. Once in liquid nitrogen, the LO-grid can be dismantled from the shuttle and stored in a suitable storage holder. Alternatively, the LO-grid can be moved directly to the holder of a TEM rod for analysis. If the grids are to be examined in an autoloader-based TEM the LO-grids are clipped into Autogrids<sup>TM</sup> (Schaffer *et al.*, 2019).

#### Results and discussion

The procedural steps of cryogenic Lift-Out are numerous and complex, with much consideration required for the geometry of the microscope in terms of stage, injectors, support grid and the lamella itself. The development of procedures and hard-

ware for lamella extraction has now yielded a technique that is capable of delivering a cryolamella to the user in a 4–6 h window (depending on sample type, hardness and dimensions of the desired lamella), similar to a manual room temperature Lift-Out. The final examination of the lamella occurs once the lamella is safely transferred into the cryo-TEM. Once in the TEM, care must be taken to limit beam sample exposure and low-dose imaging regimes are advised. Images from cryo-FIB LO lamellae (Fig. 12) are shown and demonstrate that several ultrastructural features can be observed including cell membrane (Figs. 12A–C, F), nuclear membranes (Figs. 12A, B) and mitochondria (Fig. 12C).

The images validate the applicability of the procedure to deliver cryo-lamellae of biological samples. However, it is conceded that further improvements to reduce contamination, sublimation artefacts and sample curtaining are required to routinely deliver optimal samples. The Lift-Out technique has been shown to deliver lamellae suitable for electron tomography (Mahamid *et al.*, 2015; Schaffer *et al.*, 2019).

Albeit the Lift-Out technique has been firmly established, maturing of the technique still has high importance to make the technique more straightforward, robust and repeatable. What follows are considerations regarding the hardware that may also be partially perceived as challenges for the next generation of cryolamella practitioners.

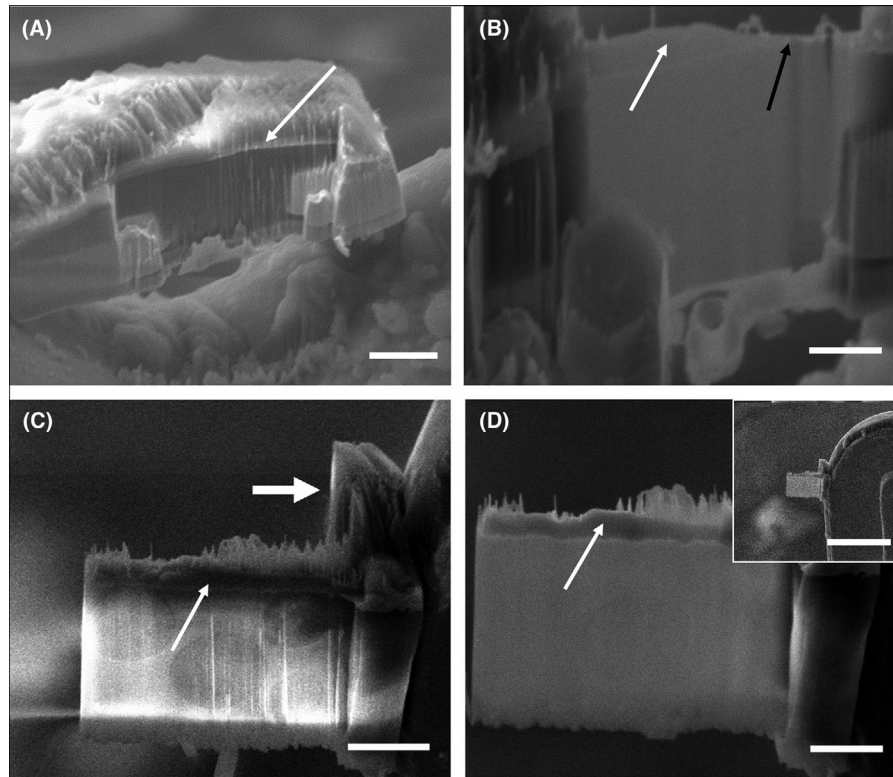


**Fig. 10.** (A) Thinning of a lamella requires sufficient coverage by Pt deposition (white arrow). (B) Latter stages of thinning. Again, note the Pt deposition (white arrow) and an area where the deposition has been eroded away (black arrow), leading to curtaining artefacts. (C) Thinning a lamella of yeast with the LO-grid post on the right. The blob of ice deposition that secures the lamella to the post is left untouched by the FIB (thick white arrow). (D) Electron transparency is reached with the Pt deposition layer still intact. (white arrow). The inset shows the lamella in relation to the LO-grid post. Scale bars (A) 4  $\mu\text{m}$ , (B) 5  $\mu\text{m}$ , (C) 2  $\mu\text{m}$ , (D) 4  $\mu\text{m}$  (D inset) 20  $\mu\text{m}$ .

It is important to stress that many of the hardware improvements include home-made modifications to existing commercially available hardware and long-term collaborations with instrument and hardware manufacturers, resulting in dedicated commercialised solutions (Parmenter *et al.*, 2016; Schaffer *et al.*, 2019; Kuba *et al.*, 2020). Future success in the field will be accelerated and enhanced through further examples of such effective collaboration.

#### Attachment options

Methods for attachment of the manipulator to the lamella and the lamella to the support grid (LO-grid) that have been explored so far are by the use of organometallic platinum (Rubino *et al.*, 2012), ice (water GIS) (Parmenter *et al.*, 2014; Parmenter *et al.*, 2016) and propane (Mahamid *et al.*, 2015). The organometallic platinum has the advantage of offering electrical conductivity to the lamella in addition to attaching the lamella to the support grid. Moreover, Pt deposition protects the lamella from curtaining.

In some cases, one may have concerns that the sample is being contaminated with Pt, which may be of concern

for EDS microanalysis. The water GIS does not have this issue. A disadvantage of applying water vapour in the microscope system is the long lifetime of water vapour in the microscope, which causes a layer of ice to deposit on all cold surfaces, including freshly milled lamella. Another alternative is propane. Propane was used as part of a prototype instrument (Mahamid *et al.*, 2015) but is not commercially available on FIB systems at present, due to practicality/safety concerns.

#### Cryolamella attachment to support grid

**GIS-assisted attachment.** The cryolamella can be attached to the support grid in several ways. The choice of which depends on the type of analysis planned for the TEM and the configuration of the cryo-FIB-SEM microscope. The lamella can be attached to the side of a post, on top of a post, or in a v-shaped post (Fig. 13A). Furthermore, it is possible to pre-mill a support grid prior to attaching of the lamella (Fig. 14). Part of the consideration involves the position of the hardware within the microscope, that is the micromanipulator and the GIS.



**Fig. 11.** Summary of the steps involved in performing a cryogenic Lift-Out, colour coded to highlight sample loading/unloading (lilac), platinum sputter coating (indigo), stage movements (green), GIS depositions (orange), manipulator movements and GIS insertions/retractions (red) and milling steps (blue). \*Sputter coating takes place in a preparation chamber if using Quorum system, if using other cryostages the location of sputtering and order of steps may vary.

GIS deposition (Pt dep, water) in cryomode is not spatially specific, unlike when performed at room temperature (Pt dep). Hence the precise deposition onto the corners of the lamella is not possible. Despite this limitation, successful attachment of a lamella has been demonstrated using the standard Pt deposition (Rubino *et al.*, 2012) and water deposition (Parmenter *et al.*, 2016) to secure the lamella in the ‘V’ of a LO-grid post (Figs. 9D–F).

The relevance of the configuration of the hardware is illustrated in Figure 13. Figure 13(B) shows the water GIS and the micromanipulator located on the same side of the chamber. Testing proved this configuration less routinely successful in comparison to having the water GIS on the opposite site to the manipulator (Figs. 13C,D). Mounting a GIS from the opposite side to the manipulator takes advantage that the port is at a lower angle, thus deposition is more from the side of the lamella/LO-grid.

The optimal configuration depends on the specific LO-grids being used. Ideally, a clear line of sight should be present between the nozzle of the GIS and the lamella being attached. In the case, where the manipulator and the GIS approach the LO-grid from opposite sides, shadowing of the lamella by surrounding posts rendered the water deposition ineffective (Fig. 13C).

Swapping a GIS from one port to another may not be a practical solution. A simple solution avoiding shadowing is attaching the lamella to the left side of far-left post (Fig. 13D). This straightforward solution is proven reproducible and simple (Fig. 10D).

It should also be noted the distance of the GIS from the post/lamella influences the rate of deposition. If the GIS is too close, the condensation of the gas leads to an uncontrolled ‘overdeposition’. Hence, it is advised to run test experiments in order to find the correct distances (by moving the z-axis of the stage or position of the GIS) and timing (duration of opening the nozzle).

*Attachment by redeposition.* An alternative to using gas-assisted deposition (Pt, water) is making use of so-called ‘redeposition’. FIB milling of the LO-grid releases material from the LO-grid. Some of this material redeposits back on the LO-grid (i.e. redeposition). It has been demonstrated that redeposition can be used to weld the lamella to the LO-grid (Kuba *et al.*, 2020). As with platinum deposition, using redeposition from the support grid, for example copper, imposes the risk of contaminating the lamella. The risk of contamination is strongly reduced when the lamella is further thinned down to electron transparency after the welding.

*Mounting position.* When a lamella is fixed in a V-shaped post, final FIB-thinning is likely causing contamination on the lamella from redeposited post material. Redeposition occurs when the FIB hits the LO-grid below the lamella, effectively starting to mill into the LO-grid. This happens when the timing for the milling is too long or from FIB ions being forward deflected from the lamella’s surface into the LO-grid. In particular when the atomic composition is determined in the TEM, contamination should be avoided as much as possible and a side attachment is preferred.

Side post attachment may, however, not be an ideal choice for techniques such as tomography. The stability of the lamella (which is only attached on one side) is insufficient

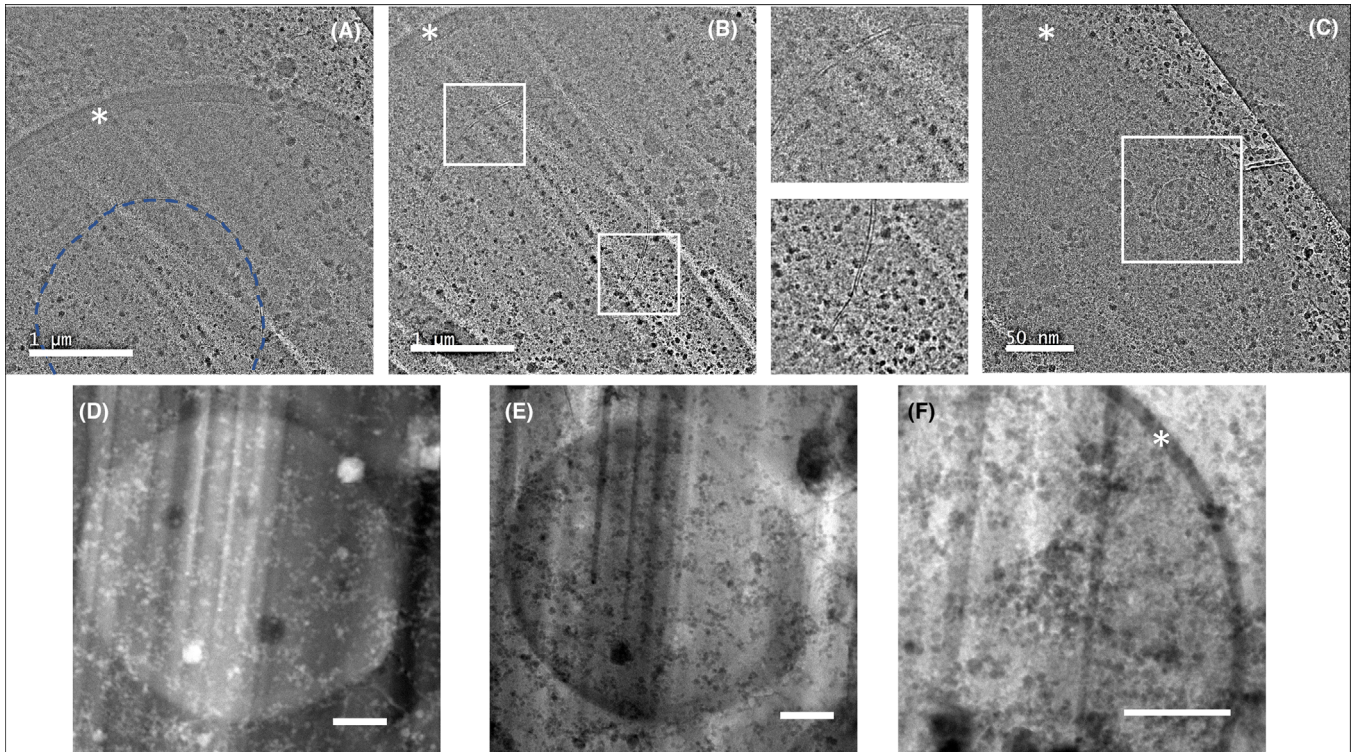


**Fig. 12.** TEM/Scanning Transmission Electron Microscope (STEM) micrographs resulting from cryo-LO work demonstrated using yeast (*S. cerevisiae*). All images were acquired at 200 kV. Bright-field TEM images show cell membranes indicated with asterisks (A)–(C), nuclear membrane outlined in blue (A) nuclear membranes in white boxes, shown as insets (B) and mitochondria highlighted in white box (C). (D) A dark-field STEM image of yeast with surface contamination visible as tiny light circles/particles. (E)–(F) bright-field STEM images with contamination visible as tiny dark circles/particles. (F) Cell membrane indicated by asterisk. Curtaining and contamination are visible in all images. Scale bars (A)–(B) 1  $\mu\text{m}$ , (C) 50 nm, (D)–(F) 1  $\mu\text{m}$

for the repeated imaging associated with tomographic serial acquisition in the TEM. Additionally, in the case of tomography, the support grid post potentially obscures the lamella for higher tilt angles.

The alternative ‘pocket’ approach was originally published by Mahamid *et al.* (2015) and recently refined by Schaffer *et al.* (2019) demonstrated using the Kleindiek cryogripper solution. Figure 14 illustrates the steps involved in preparation and its use with the Omniprobe solution. The process is performed at room temperature and consists of prefabrication (Fig. 14A) and the addition of platinum ‘shoulders’ to the top of the LO-grid post (Fig. 14C) by ion beam-induced deposition (FIB deposition). This is followed by FIB-milling of ‘pockets’ into top of the shoulders and the LO-grid to give a slot into which the lamella can be inserted (Figs. 14D–F). This allows for a lamella to be firmly attached while still being visible in the cryo-TEM at high-tilt angles. The pocket approach is a good example of the freedom in choosing a suitable geometry fitting a specific application and its corresponding need for specific cryo-TEM analyses. The platinum shoulder pillars can be made taller for more secure holding as in the original paper by Schaffer.

#### *Cryorotation stages*

Cooling devices (plastic tubes or metal braids) and electrical connections strongly limit the freedom of rotation of the cryostage to a few degrees at most. Cryorotation stages have been in development since the early 2000s, however, with few examples commercially available. The most notable commercial cryorotation stage developed beyond the prototype stage is the FEI/Quorum rotation stage used in Martinsried (Max Planck Institute for Biochemistry, Martinsried, Germany). More recently Quorum Technologies and FEI/ThermoFisher have developed stages separately as commercial offerings.

Regardless of the design, the benefits of the rotating stage are:

- (1) The alignment to a specific feature to be lifted out. This is important as, typically, the lamella is orientated along the tilt axis of the stage.
- (2) The ability to mill and observe both sides of a lamella, thus checking the progress of a lamella preparation. This includes checking the progress of the crucial undercut by being able to see all sides of the lamella and surrounding trenches.

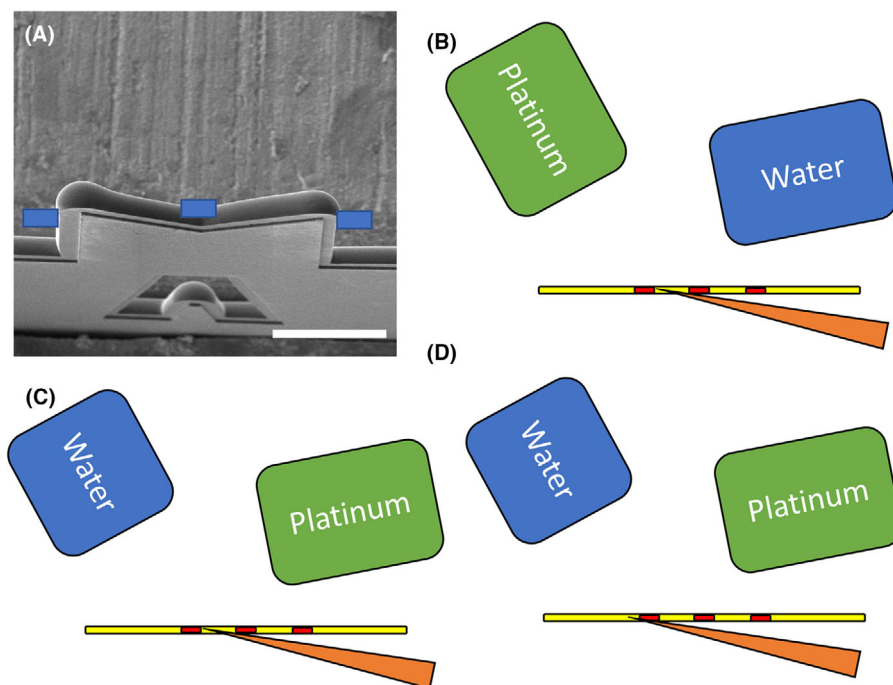


**Fig. 13.** (A) SEM image of a V-shaped post showing possible attachment locations on either side and in the 'V'. (B)–(D) Schematics of the Water GIS and Pt GIS in relation to the manipulator and the LO-posts. The schematic shows how line of sign is important when attaching the lamella to the left or right of a post.

- (3) Deposition of GIS gasses at multiple angles to provide extra security to lamellae, minimising loss during transfer.

A cryorotation stage should be considered an essential part of any future cryo-FIB systems.

#### *Critical risk points/improvements to the technique*

The transfer process of a prepared lamella to the cryo-TEM carries the biggest risk to the successful completion of the cryo-LO workflow. In the following sections, we will address all the critical risk points encountered during the transfer procedure. Across the literature, researchers have succeeded in reducing the critical risk points to a minimum, resulting in increased success rates in performing cryo-TEM investigations on cryolamellae. Nevertheless, awareness and cautiousness of the critical risk points are vital when attempting to reproduce earlier achievements.

**Sample devitrification/sublimation.** Vitrification of hydrated Life Science samples is crucial in order to preserve the structures down to the macromolecular complexes level (Hayles *et al.*, 2020). Vitrification slows down water molecules into a solid phase. The vitrification process must be extremely fast in order to prevent the formation of hexagonal ice crystals. The ice crystal formation and the related local dehydration and solute segregation are the source of the damage. Vitreous status

is maintained below  $-140^{\circ}\text{C}$ . The lamella will devitrify when the temperature rises above  $-140^{\circ}\text{C}$ , which is often recognised by cryo-TEM diffraction showing diffuse rings of a cubic phase.

Modern cryostages can maintain a sample at a desired temperature ( $-140^{\circ}\text{C}$  to  $-190^{\circ}\text{C}$ ), if the sample is well secured to the stage. The latter is not trivial. A large multicomponent stage risks inefficient cooling across all metal–metal contacts. Therefore, it is advised to make stages and sledges from one piece of metal as much as possible.

Bearing this in mind, it is sensible to require a cooled probe or gripper to operate below  $-140^{\circ}\text{C}$ . Currently, commercial solutions claim temperatures below  $-150^{\circ}\text{C}$ . It is also critical that the temperature of other surfaces in the microscope, specifically the anticontamination plate, is approximately  $20^{\circ}\text{C}$  colder. A differential temperature reduces the water vapour pressure. A lower water vapour pressure reduces contamination on the surface of the cryo-TEM lamella. However, a too low temperature on the anti-contaminator, that is a too low water vapour pressure will sublime water from the lamella, potentially affecting the lamella (Hayles *et al.*, 2020).

This is also true once the lamella has been fixed onto the support grid. If the support grid is not properly cooled, the lamella is likely to devitrify or even completely sublime.

Transfer out of the SEM chamber is the other obviously risky point where devitrification may occur. Ideally, the sledge

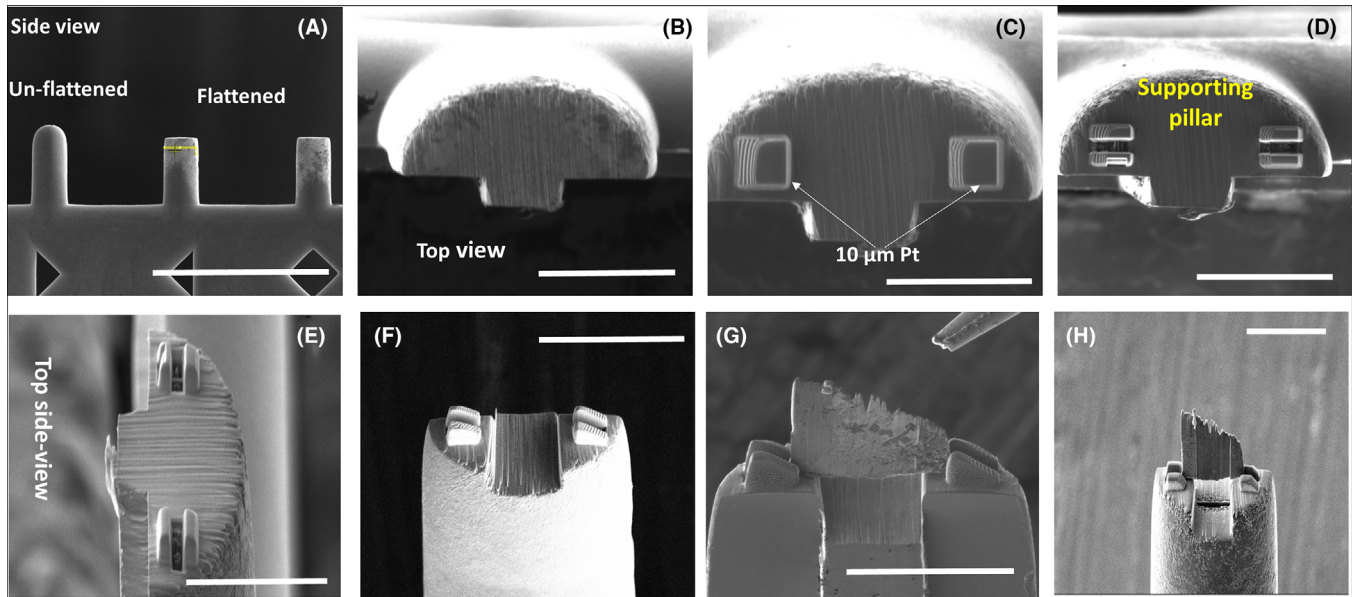


**Fig. 14.** Images of the (A), (B) bulk milling, (C) platinum deposition and (D)–(F) slot milling steps to produce ‘pockets’ on a LO-grid. (G) Demonstration images of lamella deposition and (H) the thinned lamella. Scale bars (A) 400  $\mu\text{m}$ , (B) 40  $\mu\text{m}$ , (C) 30  $\mu\text{m}$ , (D) 40  $\mu\text{m}$ , (E) 40  $\mu\text{m}$ , (F) 50  $\mu\text{m}$ , (G) 40  $\mu\text{m}$ , (H) 50  $\mu\text{m}$ .

containing frozen sample material and the lamella are kept under vacuum condition or in liquid nitrogen. Not all transfer devices allow for active cooling of the sledge. Although the vacuum condition is maintained, the mass of the sledge can maintain its low temperature only for a short time. Therefore, it is important to execute the transfer swiftly.

**Contamination.** Although it appears trivial, we must stress that the transfer routine is carried out properly in order to prevent contamination, as discussed more extensively by Hayles & De Winter (2020). Proper handling of the lamella includes using prewarmed/dry tools (to discourage moisture absorption) and frost-free (dry) liquid nitrogen. In general, wherever possible low humidity or air-free transfers should be encouraged, as this will translate to low-contamination aggregation. Freshly dispensed liquid nitrogen into a clean dry Dewar is important at all points where the lamella will see liquid nitrogen. It is always advised to keep the liquid nitrogen covered (by a loose lid) and only fill the liquid nitrogen cup shortly before the transfer. Once the transferred is successfully made, throw out the liquid nitrogen and use a hairdryer to warm up the cup and other components in the cup to drive away the condensed water. Images in Figure 15 demonstrate the progressive build-up of contamination on a Lift-Out support grid over 25 min during multiple transfers. Following the second transfer (Figs. 15D, E) both posts show significant contamination clearly demonstrating that retaining nitrogen for more than 15–20 min is inadvisable. This type of liquid nitrogen-born contamination can easily block the site of interest on the lamella, rendering hours of work ruined.

**Handling issues.** Many approaches in the cryo-FIB toolkit have meant modifications to existing hardware in order to meet the challenges of sample orientation and dimensions in both the FIB-SEM and TEM collectively. Approaches to ‘on-grid-thinning’ techniques used a modified TEM cartridge (Autogrid) loading system (Rigort *et al.*, 2012; Schaffer *et al.*, 2015) to deal with the milling angles, imaging angles and the fundamental issue of handling the TEM grids by virtue of the robust nature of the Autogrid cartridge.

Lift-Out grids are typically made of copper and have dimensions of 1.5 mm  $\times$  3 mm (half the size of a TEM grid). LO-grids are fragile and therefore manual handling with tweezers underneath liquid nitrogen requires practice. A wrong move with the tweezers can easily result in loss or damage to the lamella. Although overnight storage (or longer) is best done in dedicated cryo-TEM boxes, the retrieval of a half-grid can be difficult without damaging them. Mahamid *et al.* (2015) proposed the use of loading the half-grid into an autoloader cartridge and indeed this is the preferred solution proposed by Kuba *et al.* (2020). Direct attachment of the lamella to a pre-clipped autoloader grid reduces risk of sample loss, however, this solution is only suited to a TEM with autoloader and is not compatible with a cryo-TEM with a side-entry.

Side-entry holders impose an additional challenge, as half-grids easily fall through the hole in the cryo-TEM rod ( $\sim$ 3 mm). Proposed solutions include the use of a slot grid below the LO-grid to reduce the risk of the LO-grid falling through. It must be noted that aligning the two grids, such that the posts of the LO-grid can be seen in the TEM (in the slot area) adds extra complexity and time during transfers.

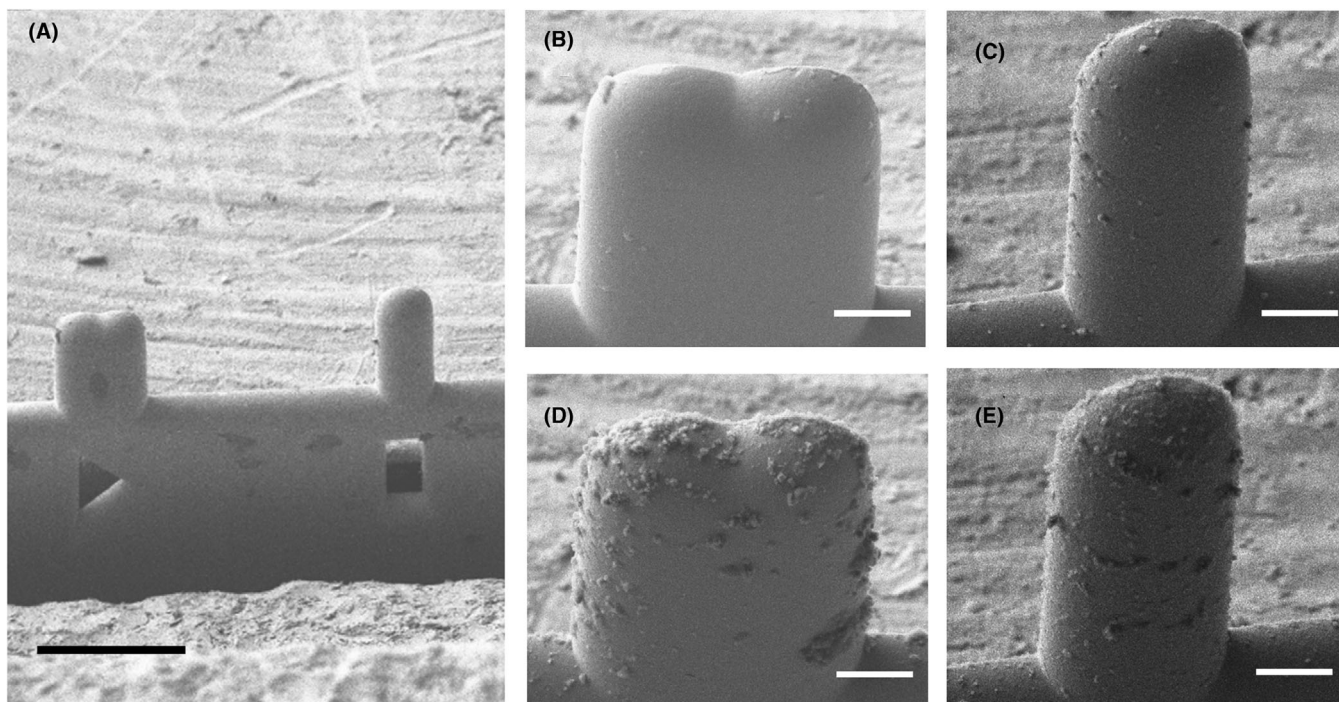


**Fig. 15.** (A) A clean/dry LO-grid was imaged prior to transfer to liquid nitrogen. (B), (C) The grid was transferred to LN<sub>2</sub> and immediately transferred back to the cryostage for reimaging. (D), (E) This procedure was repeated for a second time. Total time elapsed was 25 min indicating that the nitrogen had become contaminated by absorbed frost from first to second transfer. Scale bars (A) 100 μm, (B)–(E) 30 μm.

To minimise handling the Lift-Out grid, the slot and half grids can be prealigned and glued together in advance of the LO-procedure (Fig. 16). This ‘one piece’ solution not only solves the risk of falling through but adds a robust rim for handling the grid away from the posts in the centre of the half grid. An opening is cut in the slot grid, allowing the micromanipulator to reach the half-grid to mount the lamella (Fig. 16B). The solution with the combined grids solves the main issues described.

Further minimisation of handling LO-grids was done by gluing the grid to the retaining ring (clip ring) of a modified Gatan 626 side-loading rod (Fig. 16C). This solution required the design of a cryosledge that accepts this modified clip ring in a vertical orientation (Fig. 16D) (for deposition and milling) and allows quick transfer of the clip-ring to the cooled cryo-TEM holder. The result was a noticeable lack of frost on the LO-grid posts (Figs. 16E, F) which is attributed to the rapid transfer of the grid from FIB-SEM holder to cryo-TEM holder (around 5–10 s) meaning less exposure to frost in nitrogen.

#### *Multiple lamella extraction*

Room temperature lamella preparation is sometimes performed in batches (often automated) to yield multiple locations for Lift-Out. In order to achieve this same level of capability under cryoconditions, multiple transfers of

lamellae/repeated transfer from the same sample need to be addressed, which is more challenging for cryosystems.

There are several points to consider:

- (1) Loading of the sample and Lift-Out support grid on the same sledge, meaning that multiple extractions and depositions can be achieved to be done in one session all on the same sledge. Important is the order of the sequence (i.e. milling, lift-out, mounting, thinning), in particular, when using GIS-assisted mounting of the lamella. Releasing the platinum precursor gas or water vapour in the microscope chamber will contaminate all cold surfaces. An already thinned lamella will collect contamination when subsequent lamellae are mounted. Contamination from subsequent lamellae is probably less of an issue when local redeposition is being used to fix a lamella to the LO support grid. Perhaps the easiest solution is to perform the final thinning only once all the lamellae have been attached to the LO support grid.
- (2) When a Lift-Out session exceeds one day, and it becomes necessary to store a sample overnight, contamination of sample and any deposited lamellae could be a significant issue. It is advised to store the sample in the microscope chamber and maintain the cryoconditions overnight. Again, it is advised to perform the final thinning only shortly before making the transfer to the cryo-TEM and thus not before overnight storage.

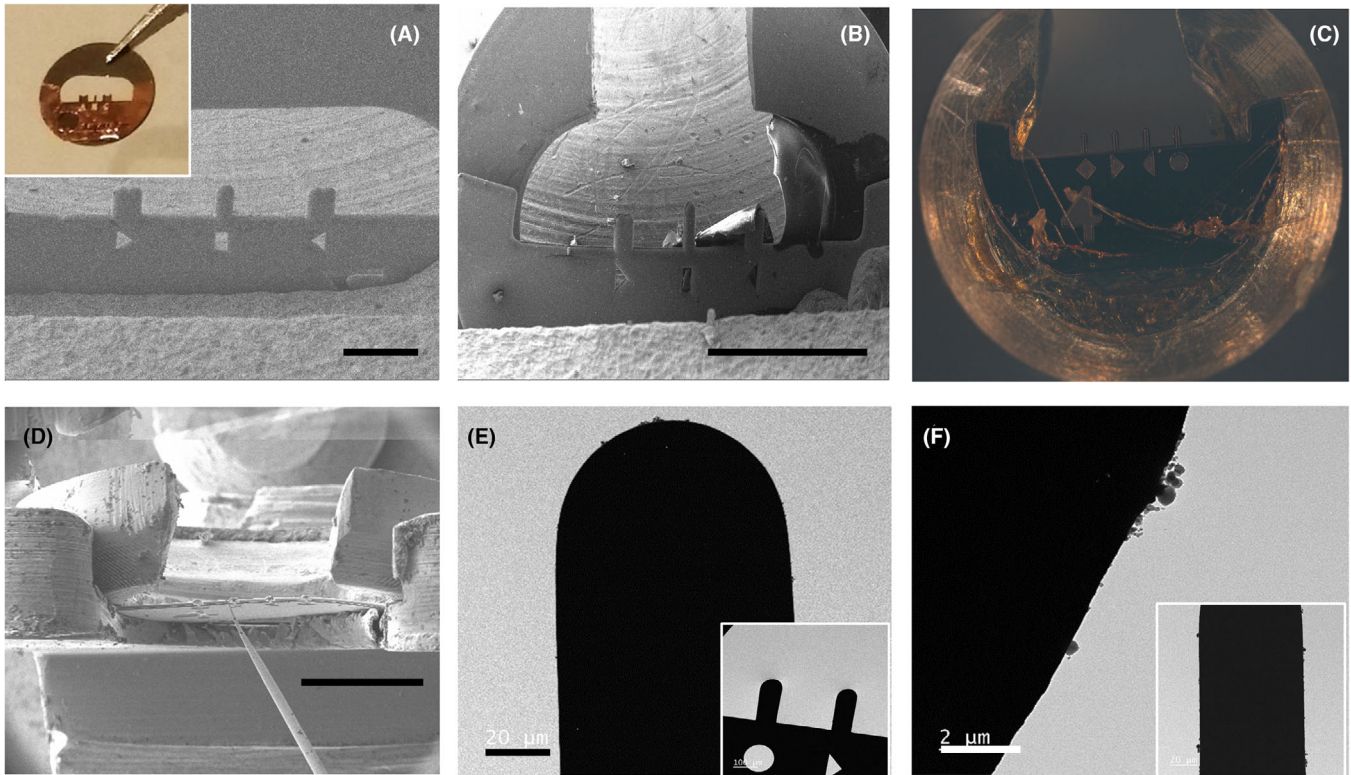


**Fig. 16.** The evolution of LO-grid transfer to cryo-TEM. (A) Originally proposed solution to 'one-piece' handling of the LO-grid. (B) Modified solution with to allow manipulator access. (C) Direct attachment of a LO-grid to the modified Gatan 626 'clip-ring'. (D) Micrograph of the clip-ring, LO-grid and the Omniprobe. (E), (F) Cryo-TEM images of posts with minimal frost visible. Scale bars (A) 300  $\mu\text{m}$ , (B), (D) 1 mm, (E) 20  $\mu\text{m}$ , (F) 2  $\mu\text{m}$ .

- (3) An additional issue with performing a series of extractions from the same sample, if using gas deposition, is the resulting cryo-condensed layer (Pt or water) that can rapidly build up on the surface of the sample. This could obscure the area of interest or cause complications when extracting the second (or third) lamella. There will also be a build-up of the condensation layer on the micromanipulator; however, this layer can be removed by exposing the 'needle' to the FIB for a few minutes (Fig. 17). Additional time for this step should be factored into the overall time demands of the procedures.

### Conclusions and future

Interest in the technique of cryo-FIB LO has gained momentum in recent years as publications show that it can be successfully achieved and its applications to biological samples in a fully hydrated state are demonstrated. The library of examples currently stands at cultured cells, eukaryotes and spores.

It should be recognised that cryo-LO has been demonstrated on what one could consider 'materials systems' including semiconductors and copper (Antoniou *et al.*, 2012), hydrogels (Zachman *et al.*, 2016) and battery electrolytes (Zachman *et al.*, 2018).

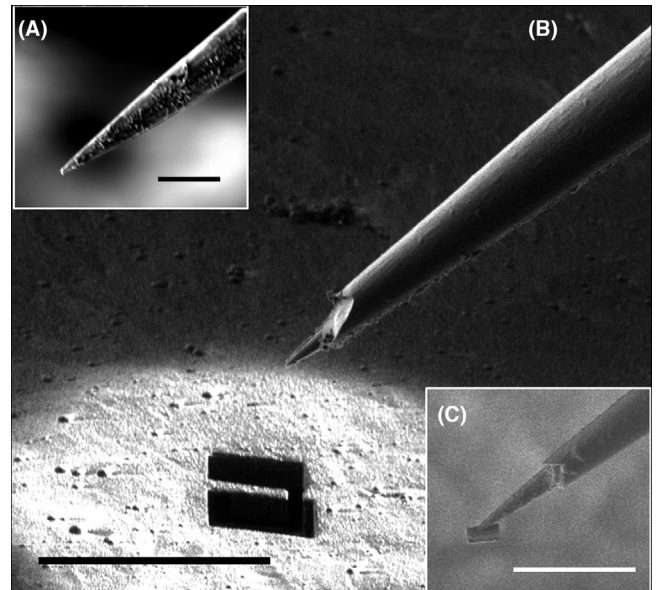


**Fig. 17.** Using the FIB to regenerate a sharp micromanipulator tip. (A) Prior to cleaning. (B) Cleaned and approaching the next lamella. (C) A second successfully extracted lamella using this regenerated tip. Scale bars (A) 10  $\mu\text{m}$  (B) 50  $\mu\text{m}$  (C) 100  $\mu\text{m}$ .

The focus of this paper has been on transfer to cryo-TEM; however, it should not be overlooked that cryo-Lift-Out and transfer to other advanced instrumentation is possible. Subject to solving handling and geometry requirements of those instruments include but are not limited to cryo-Atom Probe (Schreiber *et al.*, 2018), Soft X-Ray tomography or X-ray 3D ptychography (unpublished work).

The future is bright for Cryo-LO to follow ‘on-grid-thinning’ for TEM preparation, but excitingly also for other applications of cryo-Lift-Out for non-EM purposes.

## Acknowledgements

The authors would like to acknowledge funding from the University of Nottingham RPA, Bridging the Gaps scheme (Nottingham), the HERMES Fellowship (Nottingham), the EPSRC under grants EP/L022494/1 and EP/R025282/1. Many thanks to Mike Hayles, Alex Rigort, Bob Morrison, Greg Moldovan, Cheryl Hartfield, Gonzalo Amador, Julie Watts, Mike Fay and Miroslava Schaffer for many fruitful technical discussions and their input to this exciting and challenging area of science/technical work. Many thanks go to staff at Oxford Instruments, Quorum Technologies and the nmRC (Nottingham). In particular, the authors would like to thank the continued support of this work given by Andrei Khlobystov and Paul Brown. The authors would also like to recognise the work of Tommy Napier and David Laird (Physics workshop) for technical and workshop support at the University of Nottingham. A special thanks go to Matthijs de Winter for help with formatting, style and manuscript preparation and for guest editing the special issue.

## References

- Antonioni, N., Graham, A., Hartfield, C., Amador, G. & Int, A.S.M. (2012) *Failure Analysis of Electronic Material Using Cryogenic FIB-SEM*, pp. 399–405. ASM International, Materials Park.
- De Winter, D.A.M., Hsieh, C., Marko, M. & Hayles, M.F. (2020) Cryo-FIB preparation of whole cells and tissue for cryo-TEM: use of high-pressure frozen specimens in tubes and planchets. *J. Microsc.* <https://doi.org/10.1111/jmi.12943>.
- Dubochet, J. (2007) The physics of rapid cooling and its implications for cryoimmobilization of cells. *Methods in Cell Biology* (ed. by J.R. McIntosh), Vol 79, pp. 7–21. Elsevier/Academic Press, Amsterdam.
- Dubochet, J., Zuber, B., Eltsov, M., Bouchet-Marquis, C., Al-Amoudi, A. & Livolant, F. (2007) How to “read” a vitreous section. *Methods in Cell Biology* (ed. by J.R. McIntosh), Vol 79, pp. 385–406. Elsevier/Academic Press, Amsterdam.
- Edwards, H.K., Fay, M.W., Anderson, S.I., Scotchford, C.A., Grant, D.M. & Brown, P.D. (2009) An appraisal of ultramicrotomy, FIBSEM and cryogenic FIBSEM techniques for the sectioning of biological cells on titanium substrates for TEM investigation. *J. Microsc.* **234**(1), 16–25.
- Giannuzzi, L.A., Drown, J.L., Brown, S.R., Irwin, R.B. & Stevie, F. (1998) Applications of the FIB lift-out technique for TEM specimen preparation. *Microsc. Res. Tech.* **41**(4), 285–290.
- Giannuzzi, L.A., Yu, Z.Y., Yin, D. *et al.* (2015) Theory and new applications of ex situ lift out [article]. *Microsc. Microanal.* **21**(4), 1034–1048.
- Han, H.M., Zuber, B. & Dubochet, J. (2008) Compression and crevasses in vitreous sections under different cutting conditions [Article]. *J. Microsc.* **230**(2), 167–171.
- Hayles, M.F. & de Winter, D.A.M. (2020) An introduction to cryo-FIB-SEM cross-sectioning of frozen, hydrated Life Science samples. *J. Microsc.* <https://doi.org/10.1111/jmi.12951>.
- Hayles, M.F., Matthijs de Winter, D.A., Schneijdenberg, C.T.W.M. *et al.* (2010) The making of frozen-hydrated, vitreous lamellas from cells for cryo-electron microscopy. *J. Struct. Biol.* **172**(2), 180–190.
- Hayles, M.F., Stokes, D.J., Phifer, D. & Findlay, K.C. (2007) A technique for improved focused ion beam milling of cryo-prepared life science specimens. *J. Microsc.* **226**(3), 263–269.
- Hsieh, C., Schmelzer, T., Kishchenko, G., Wagenknecht, T. & Marko, M. (2014) Practical workflow for cryo focused-ion-beam milling of tissues and cells for cryo-TEM tomography [Article]. *J. Struct. Biol.* **185**(1), 32–41.
- Krueger, R. (1999) Dual-column (FIB-SEM) wafer applications [Review]. *Micron* **30**(3), 221–226.
- Kuba, J., Mitchels, J., Hovorka, M. *et al.* (2020) Advanced cryo-tomography workflow developments – correlative microscopy, milling automation and cryo-lift-out. *J. Microsc.* <https://doi.org/10.1111/jmi.12939>.
- Li, J., Malis, T. & Dionne, S. (2006) Recent advances in FIB-TEM specimen preparation techniques. *Mater. Charact.* **57**(1), 64–70.
- Livesey, S.A., Delcampo, A.A., McDowall, A.W. & Stasny, J.T. (1991) Cryofixation and ultra-low-temperature freeze-drying as a preparative technique for TEM [Article]. *J. Microsc.* **161**, 205–215.
- Mahamid, J., Schampers, R., Persoon, H., Hyman, A.A., Baumeister, W. & Plitzko, J.M. (2015) A focused ion beam milling and lift-out approach for site-specific preparation of frozen-hydrated lamellas from multicellular organisms. *J. Struct. Biol.* **192**(2), 262–269.
- Marko, M., Hsieh, C., Moberlychan, W., Mannella, C.A. & Frank, J. (2006) Focused ion beam milling of vitreous water: prospects for an alternative to cryo-ultramicrotomy of frozen-hydrated biological samples. *J. Microsc.* **222**(1), 42–47.
- Marko, M., Hsieh, C., Schalek, R., Frank, J. & Mannella, C. (2007) Focused-ion-beam thinning of frozen-hydrated biological specimens for cryo-electron microscopy [Article]. *Nat. Methods* **4**(3), 215–217.
- Moor, H. (1987) Theory and practice of high pressure freezing. *Cryotechniques in Biological Electron Microscopy* (ed. by R.A.Z.K. Steinbrecht), pp. 175–191. Springer, Berlin, Heidelberg.
- Parmenter, C., Fay, M., Hartfield, C. & Amador, G., Moldovan, G. (2014) Cryogenic FIB lift-out as a preparation method for damage-free soft matter TEM imaging. *Microsc. Microanal.* **20**(S3), 1224–1225.
- Parmenter, C.D.J., Fay, M.W., Hartfield, C. & Eltahir, H.M. (2016) Making the practically impossible “Merely difficult” – cryogenic FIB lift-out for “damage free” soft matter imaging. *Microsc. Res. Tech.* **79**(4), 298–303.
- Reipert, S., Fischer, I. & Wiche, G. (2003) Cryofixation of epithelial cells grown on sapphire coverslips by impact freezing [Article]. *J. Microsc.-Oxf.* **209**, 76–80.
- Rigort, A., Bäuerlein, F.J., Leis, A. *et al.* (2010) Micromachining tools and correlative approaches for cellular cryo-electron tomography. *J. Struct. Biol.* **172**(2), 169–179.
- Rigort, A., Bäuerlein, F.J.B., Villa, E. *et al.* (2012) Focused ion beam micromachining of eukaryotic cells for cryoelectron tomography. *Proc. Nat. Acad. Sci.* **109**(12), 4449–4454.

- Rigort, A. & Plitzko, J.M. (2015) Cryo-focused-ion-beam applications in structural biology [Review]. *Arch. Biochem. Biophys.* **581**, 122–130.
- Rubino, S., Akhtar, S., Melin, P., Searle, A., Spellward, P. & Leifer, K. (2012) A site-specific focused-ion-beam lift-out method for cryo transmission electron microscopy. *J. Struct. Biol.* **180**(3), 572–576.
- Schaffer, M., Engel, B.D., Laugks, T., Mahamid, J., Plitzko, J.M. & Baumeister, W. (2015) Cryo-focused ion beam sample preparation for imaging vitreous cells by cryo-electron tomography. *Bio-protocol* **5**(17), e1575. <https://doi.org/10.21769/BioProtoc.1575>.
- Schaffer, M., Pfeffer, S., Mahamid, J. *et al.* (2019) A cryo-FIB lift-out technique enables molecular-resolution cryo-ET within native *Caenorhabditis elegans* tissue. *Nat. Methods*. **16**(8), 757–762.
- Schreiber, D.K., Perea, D.E., Ryan, J.V., Evans, J.E. & Vienna, J.D. (2018) A method for site-specific and cryogenic specimen fabrication of liquid/solid interfaces for atom probe tomography. *Ultramicroscopy* **194**, 89–99.
- Sivel, V.G.M., Van den Brand, J., Wang, W.R. *et al.* (2004) Application of the dual-beam FIB/SEM to metals research [Article; Proceedings Paper]. *J. Microsc. – Oxf.* **214**, 237–245.
- Tivol, W.F., Briegel, A. & Jensen, G.J. (2008) An improved cryogen for plunge freezing. *Microsc. Microanal.* **14**(5), 375–379.
- Umrath, W. (1974) Cooling bath for rapid freezing in electron microscopy. *J. Microsc.* **101**(1), 103–105.
- Zachman, M.J., Asenath-Smith, E., Estroff, L.A. & Kourkoutis, L.F. (2016) Site-specific preparation of intact solid–liquid interfaces by label-free in situ localization and cryo-focused ion beam lift-out. *Microsc. Microanal.* **22**(6), 1338–1349.
- Zachman, M.J., Tu, Z., Choudhury, S., Archer, L.A. & Kourkoutis, L.F. (2018) Cryo-STEM mapping of solid-liquid interfaces and dendrites in lithium-metal batteries. *Nature* **560**(7718), 345–349.